# Mapping the sensitivity of split ring resonators using a localized analyte

Sharpe, Graham J.; Vilhena, Henrique; Lahiri, Basudev; McMeekin, Scott; De La Rue, Richard M.; Johnson, Nigel P.

*Published in:*
Applied Physics Letters

*DOI:*
10.1063/1.4954797

*Publication date:*
2016

*Document Version*
Publisher's PDF, also known as Version of record

AIP | Applied Physics Letters

# Mapping the sensitivity of split ring resonators using a localized analyte

Graham J. Sharp, Henrique Vilhena, Basudev Lahiri, Scott. G. McMeekin, Richard M. De La Rue, and Nigel P. Johnson

Citation: Applied Physics Letters **108**, 251105 (2016); doi: 10.1063/1.4954797
View online: http://dx.doi.org/10.1063/1.4954797
View Table of Contents: http://scitation.aip.org/content/aip/journal/apl/108/25?ver=pdfcov
Published by the AIP Publishing



# Mapping the sensitivity of split ring resonators using a localized analyte

Graham J. Sharp,[1] Henrique Vilhena,[2] Basudev Lahiri,[1] Scott. G. McMeekin,[2] Richard M. De La Rue,[1] and Nigel P. Johnson[1,a)]
[1]*Optoelectronics Research Group, School of Engineering, University of Glasgow, Glasgow G12 8LT, United Kingdom*
[2]*Department of Engineering, Glasgow Caledonian University, Glasgow G4 0BA, United Kingdom*

(Received 22 April 2016; accepted 14 June 2016; published online 23 June 2016)

Split ring resonator (SRR) based metamaterials have frequently been demonstrated for use as optical sensors of organic materials. This is made possible by matching the wavelength of the SRR plasmonic resonance with a molecular resonance of a specific analyte, which is usually placed on top of the metal structure. However, systematic studies of SRRs that identify the regions that exhibit a high electric field strength are commonly performed using simulations. In this paper we demonstrate that areas of high electric field strength, termed "hot-spots," can be found by localizing a small quantity of organic analyte at various positions on or near the structure. Furthermore, the sensitivity of the SRR to the localized analyte can be quantified to determine, experimentally, suitable regions for optical sensing. 
[http://dx.doi.org/10.1063/1.4954797]

Surface plasmon based optical biosensors are emerging as one of the most accurate and sensitive detection tools for the identification of minute quantities of biochemical compounds (analytes).[1–5] Detection of minute quantities of analytes is of great interest for immunosensing, diagnostics, security, and forensic applications.[1–5] Localized surface plasmon resonances (LSPRs) are collective oscillations of conduction electrons that are produced in metallic nanostructures when excited by incident light. The localization of surface plasmons allows for the concentration of light in extremely small modal volumes (~10 to $10^3$ $nm^3$) that form electromagnetic hot-spots.[6] These hot-spots are highly sensitive and are extremely susceptible to changes in external conditions, such as changes in refractive index due to the addition of an analyte within close proximity. Split-ring resonators (SRRs) are metallic nanostructures that can act as LC oscillating circuits—and their resonances can be tuned over a range of wavelengths by changing their physical dimensions and constituent metals.[7–9] It is also possible to match the plasmonic resonance of the SRRs with the molecular vibrational resonances of a selected bond in a target analyte, for enhanced detection and identification.[10–12]

In this paper we compare the accuracy and sensitivity of SRRs in probing thin films (~110 nm thick) of poly-methyl methacrylate (PMMA) that are localized as square blocks (150 nm × 150 nm) in various positions in their vicinity.

We fabricate our SRRs using a combination of electron-beam lithography (EBL), metallization, and lift-off techniques—and characterize them using standard Fourier transform infra-red spectroscopy (FTIR) tools.

The SRRs designed have a circular "C-shaped" geometry, with a diameter of 1.5 $\mu$m. They consist of a single circular metal hoop, 100 nm wide together with a small gap (~150 nm). The SRRs are designed to resonate at the mid-infrared region, specifically near the wavelength of 5 $\mu$m. This matches their plasmonic resonance with the molecular vibrational resonance of the carbonyl bond (C = O) of the PMMA at a wavelength of 5.75 $\mu$m.[13] The structures were fabricated as nano-antenna arrays with a periodicity of 2.9 $\mu$m in both x- and y-directions. Transverse electric (TE) polarized incident light and, separately, transverse magnetic (TM) polarized light was used to excite the metamaterial. The orientation of the electric field for these polarizations with respect to the SRR structure is shown in Fig. 1. In the TE configuration, the electric field couples with the capacitance of the gap in the SRR and generates a circulating current around it. This circulating current induces a magnetic field in the base of the SRRs that interacts with the external field. In previous work, we have used asymmetric SRRs (A-SRRs) for optical detection of minute quantities of PMMA, localizing square blocks of PMMA near the electromagnetic hot-spots of the A-SRRs to determine their sensitivity.[12]

SRR arrays were fabricated on a fused silica substrate using EBL. Patterns were written using a PMMA resist bi-layer and subsequent temperature controlled development in isopropyl alcohol and ultrapure water (UPW). Titanium (Ti, 5 nm) followed by gold (Au, 100 nm) was deposited by electron-beam evaporation before lift-off in warm acetone. Upon metallization of the SRR structures, a 110 nm thick film of PMMA (with a molecular weight of 84 000) was spin-coated onto the sample. Using multiple gold alignment markers, 150 nm square blocks of PMMA were patterned in specific locations relative to the SRRs by exposing the regions of PMMA that were to be removed during development. The position of the EBL patterning was aligned with the SRR structures using the metal markers and the PMMA film was selectively exposed, leaving only the 150 nm square blocks. Following development of the PMMA film, only the unexposed blocks remained, together with the metal SRRs. Experimental measurement of the SRR array (both with and without PMMA analyte) was performed using a Bruker

a)Author to whom correspondence should be addressed. Electronic mail: nigel.johnson@glasgow.ac.uk

 

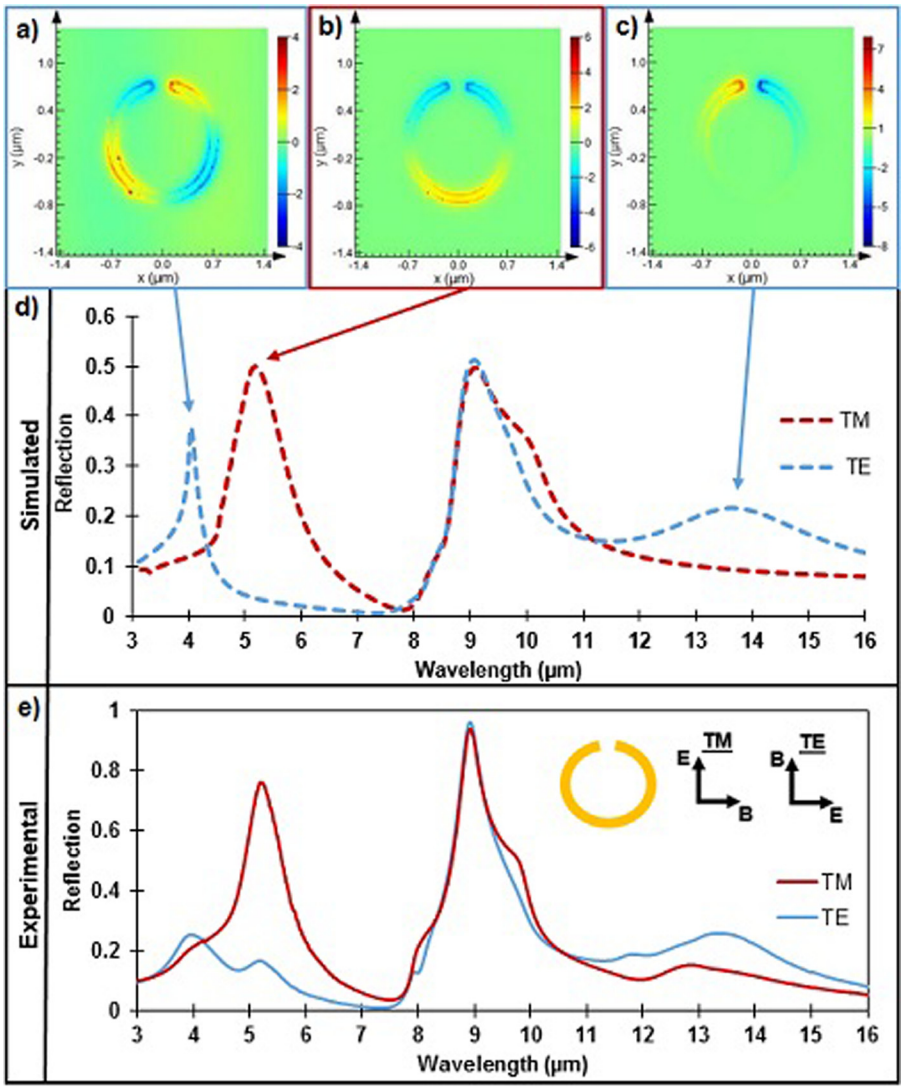


FIG. 1. (a)–(c) Simulated plots of the electric field distribution in a single unit-cell of the SRR, without any analyte present, at different wavelengths and incident polarizations. (a) Second order resonant mode under TE excitation at 4.1 $\mu$m, (b) TM resonant mode at 5.2 $\mu$m, and (c) fundamental resonant mode under TE excitation at $\sim$14 $\mu$m. (d) Simulated spectra of the SRR for TE and TM polarizations with arrows identifying peaks with respective field plots. (e) Experimental spectra of fabricated SRR, with definition of TM and TE polarizations inset.

Vertex FTIR spectrometer with Hyperion microscope. An unpatterned Au film was used as a background reference for the measurement of the nanostructure array and a ZnSe polarizer, positioned between the light source and fabricated sample, was used to control the polarization of the incident light. In order to verify the experimental measurements, finite difference time domain (FDTD) simulations of the fabricated patterns were performed using Lumerical FDTD Solutions, which also enables the electric field distribution in the SRR to be plotted. A Drude model was used to simulate the response of the SRR—and real and imaginary refractive index data from Kischkat *et al.*[14] were used to model the $SiO_2$ substrate. The behavior of PMMA was modeled using a Lorentz oscillator model. Experimental reflectance measurements of the fabricated structures, without any analyte, are shown in Fig. 1—alongside complementary simulated spectra and electric field plots at given resonant wavelengths. In all the experimental spectra presented, atmospheric $CO_2$ absorption features at 4.25 $\mu$m were reduced in magnitude, or removed, by applying a smoothing function to the measured data.

Both the experimental and simulated spectra show a number of resonance peaks, determined by the polarization of the incident light and the order of the resonant mode of the SRRs. The strong peak visible at 9 $\mu$m is caused by asymmetric stretching of Si-O-Si bands in the fused silica substrate and so is present for both TE and TM polarizations.[15] Simulations using TM polarized light incident show a strong reflectance peak at 5.27 $\mu$m while, under TE excitation, a peak is visible at 4 $\mu$m. Electric field plots of the structure at the latter wavelength indicate excitation of the second order resonant mode, with the fundamental "LC resonance" being observable at 13.5 $\mu$m. For the LC resonance the electric field component of the incident light is coupled across the gap of the split ring (TE polarization) and induces a circulating current in the metal structure. In this scenario the electric field is concentrated at the end of each arm of the split ring. The plots of both the higher order mode and the fundamental LC resonance, shown in Figs. 1(a) and 1(c), respectively, indicate that the electric field has opposing phases at either end of the metal arm at the gap. It is also noted that the electric field strength for the higher order resonance has a lower magnitude than for the LC resonance. The low level of geometrical asymmetry of the SRR leads to the strong plasmonic resonance observed at 5.27 $\mu$m under TM excitation.

Experimental measurements show a similar distribution of resonances to the simulated spectra. It is notable that the

amplitude of the TE second order resonant mode is lower in the experimental measurements than it is in the simulations, by 25% and 40%, respectively. This can be attributed to optical leakage in the ZnSe polarizer and a consequent degree of polarization (DOP) of less than 100%, resulting in the presence of both the TE second-order resonance at 4 $\mu$m and the TM excited resonance at 5.27 $\mu$m, in a single spectral plot. Small inaccuracies in the experimental alignment of the E-field using the polarizer and the near-symmetrical geometry of the structure probably also contribute. The dependence of the angle of polarization on symmetrical and near-symmetrical ring resonators has been reported previously.[16,17]

As a means of determining the impact that the quantity of analyte has on the reflectance spectra, a 110 nm film of PMMA was spin-coated over the entire SRR array. This provides a comparison with the reflectance measurements obtained from SRRs in which PMMA is localized in different positions on or near the metal structures. Fig. 2 shows the reflectance spectra (TM and TE mode) of the SRRs, when covered in a 110 nm thin film of PMMA, together with the spectra obtained from the SRRs only, without any analyte. A clear spectral red-shift is seen with the PMMA film applied—and the carbonyl bond in the PMMA produces a distinct spectral feature at 5.75 $\mu$m. The prominence of this feature increases when a plasmonic resonance from the SRRs is near in wavelength, as seen in the measurements with TM excitation and shown in Fig. 2.

The sensitivity of an SRR to PMMA is determined by the shift in the resonant wavelength from its original peak position—as well as the change in refractive index, n, of the material being sensed. It is expressed as $s = \Delta\lambda/\Delta n$, where the sensitivity is defined by $s$ and is denoted in nanometers per refractive index unit (nm/RIU).[18] The change in $n$ is, in this work, given as the difference between the refractive index of PMMA and that of air, i.e., $1.49 - 1 = 0.49$.[19] PMMA that is present within an electric field hotspot changes the inductive and capacitive components of the structure and consequently shifts resonances to longer wavelengths. In areas where the electric field strength is high, these changes are greater in magnitude—resulting in a larger $\Delta\lambda$ and, therefore, improved sensitivity.[20] Conversely, PMMA placed in regions that exhibit no electric field activity does not alter the plasmonic behavior of the metamaterial—and so is not sensed. From the spectra taken using a 110 nm thin film blanketing the SRRs, the sensitivity is calculated as 775 nm/RIU for TE incident light and 630 nm/RIU under TM excitation. This uniform thin film configuration produces a large spectral shift and subsequently high sensitivity values, because of the large refractive index change. However, the continuous thin film configuration cannot offer insight, at least experimentally, into the sensitivity attributable to specific physical regions of the metamaterial pattern, which requires local probing. Spectra obtained from the SRRs with PMMA blocks localized in their vicinity are shown in Fig. 3, with both experimental measurements and simulated results included for each PMMA position.

It is evident in both the experimental results and the complementary simulations that the region of greatest sensitivity is the gap in the SRR. TE measurements of PMMA localized at this position exhibit a spectral shift of 220 nm,

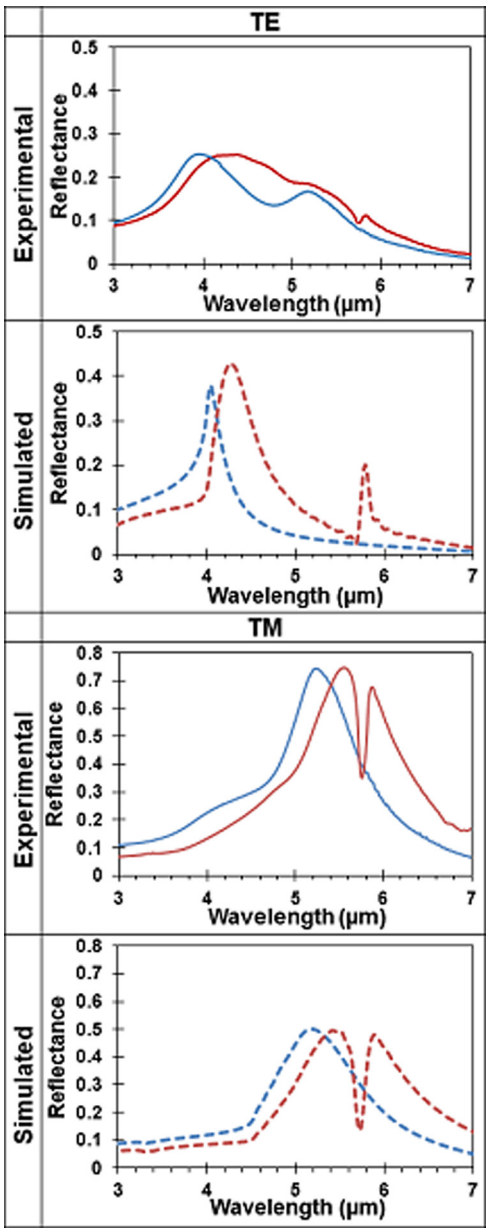


FIG. 2. Experimental and simulated reflectance spectra of the SRR array with (red) and without (blue) a 110 nm thin film of PMMA on top. Spectra are obtained using both TE and TM polarized incident light. The carbonyl absorption feature produced by the presence of PMMA is clearly visible at 5.75 $\mu$m.

resulting in a sensitivity of 449 nm/RIU. This accounts for 58% of the total sensitivity obtained under TE excitation when a 110 nm PMMA film is applied to the entire unit cell, as recorded in Fig. 2, and is despite the fact that the volume of the analyte in the localized case is approximately only 2.7% of that of the thin film. A much smaller shift of 10 nm (and sensitivity of 20 nm/RIU) is exhibited with the analyte localized in the "6 o'clock" position of the SRR, corresponding to 2.6% of the total thin film sensitivity. PMMA localized in the center of the ring fails to produce any spectral shift for either TE or TM incident light—and the SRR is effectively blind to the presence of the analyte at this location. With TE-polarized incident light, the ends of the arms at the gap of the SRR show the maximum differential in field strength, shown in Fig. 1. PMMA within the highly concentrated field provides a change of the real part of the dielectric

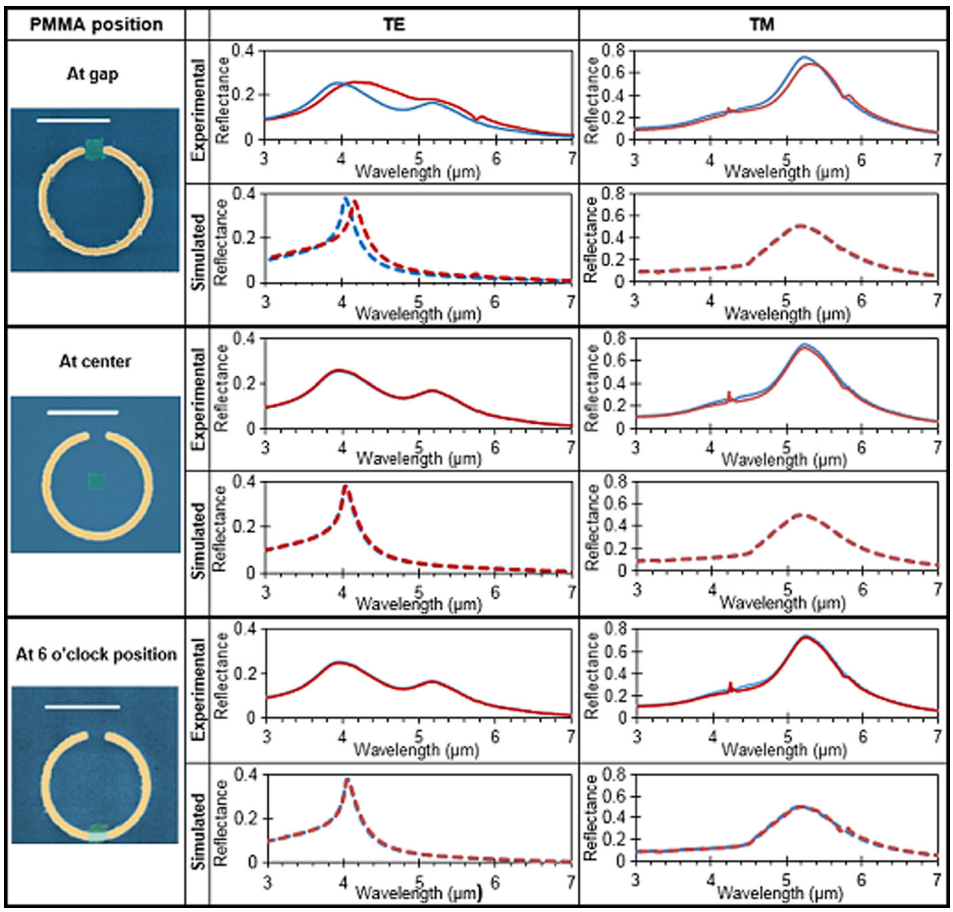


FIG. 3. Experimental and simulated spectra of the SRR array with a 150 nm by 150 nm block of PMMA (110 nm thick) localized in three different positions—at the gap of the SRR, in the center of the SRR, and at the "6 o'clock" position on the arm of the SRR. The blue plots show the spectra of the SRRs alone and red plots with localized PMMA. SEM micrographs with false color show the position of the PMMA (green) with respect to the SRR (gold) on the silica substrate (blue). The white scale bar represents a length of 1 $\mu$m.

constant and shifts the plasmonic resonance to a longer wavelength. With the PMMA located between the ends of the SRR arms the interaction between the analyte and the electric flux density is at its highest. In the center of the ring and at the "6 o'clock" position the difference in field strength is minimal and therefore the interaction between the analyte and the electric flux density is insufficient to produce a measurable shift.

An understanding of the spectral shift due to the presence of PMMA, as well as a number of experimental parameters, enables a calculation, using Eq. (1), of the minimum detectable number of molecules in the analyte[6]

$$N_a = \frac{|\Delta\omega_n|\varepsilon_d V_m}{\gamma_n \alpha Q}, \tag{1}$$

where $N_a$ is the minimum number of analyte molecules that can be sensed, $\Delta\omega_n$ is the detected frequency shift, $\gamma_n$ is the spectral width, $\varepsilon_d$ is the relative permittivity of the analyte ($\varepsilon_d = n^2$, with $\varepsilon_d$ of PMMA $= (1.45)^2$), $\alpha$ is the molecular polarizability of the PMMA analyte ($cm^3$, as defined by Naidu *et al.*[21]), $V_m$ is the modal volume of the analyte in $m^3$, and Q is the resonance quality factor of the SRR. It should be noted that, for these calculations, the molecular polarizability is assumed to be half of the value stated by Naidu *et al.*, due to the molecular weight of the localized PMMA being half that of the PMMA used in Naidu *et al.*'s experiments. After conversion from $cm^3$ to the SI unit of $m^3$, this gives a molecular polarizability value of $7.72 \times 10^{-27}\ m^3$. The modal volume of the PMMA localized at the gap is simulated with three dimensional modeling using the established criteria of $|E^2|$ being greater than $10^3$.[22] We estimate $V_m$ to be $4.29 \times 10^{-22}\ m^3$ (~1/5 of the total volume of the PMMA block). The $Q$-factor is defined as $Q = \omega_r/FWHM$, where $\omega_r$ is the resonant frequency of the SRR and FWHM is the full-width at half-maximum of the resonance. From the experimental measurements with PMMA localized at the gap of the SRR, we have calculated an $N_a$ value of 6340 detectable molecules, using the measured $Q$-factor of 3.5. With a uniform PMMA thin film applied, the $N_a$ value is calculated to be 25 260, owing to the increase in the modal volume and spectral shift.

In conclusion, this letter demonstrates that the sensitivity of "hot-spots" for SRR metamaterials can be identified and quantified experimentally, as well as by simulation. In probing specific localized regions of a unit cell of the array, the sensitivity to the presence of an analyte (in this instance PMMA) can be determined. For a single-split SRR, the region of greatest sensitivity is experimentally found to be the gap region, accounting for 58% of the total sensitivity observed from a 110 nm thin film that covers the entire unit cell.

The authors would like to acknowledge the support from the EPSRC in the form of a scholarship for G.J.S. (Grant No. EP/J500434/1). They would also like to acknowledge the facilities and staff of the James Watt Nanofabrication Centre (JWNC) at the University of Glasgow, where the structures presented in this work were fabricated.

[1]A. V. Kabashin, P. Evans, S. Pastkovsky, W. Hendren, G. A. Wurtz, R. Atkinson, R. Pollard, V. A. Podolskiy, and A. V. Zayats, Nat. Mater. **8**(11), 867 (2009).
[2]T. Chen, S. Li, and H. Sun, Sensors **12**(3), 2742 (2012).
[3]A. G. Brolo, Nat. Photonics **6**(11), 709 (2012).
[4]C. Wu, A. B. Khanikaev, R. Adato, N. Arju, A. A. Yanik, H. Altug, and G. Shvets, Nat. Mater. **11**(1), 69 (2012).
[5]V. Liberman, R. Adato, T. H. Jeys, B. G. Saar, S. Erramilli, and H. Altug, Opt. Express **20**(11), 11953 (2012).
[6]M. I. Stockman, Phys. Today **64**(2), 39 (2011).
[7]J. Zhou, T. Koschny, M. Kafesaki, E. N. Economou, J. B. Pendry, and C. M. Soukoulis, Phys. Rev. Lett. **95**(22), 223902 (2005).
[8]M. W. Klein, C. Enkrich, M. Wegener, C. M. Soukoulis, and S. Linden, Opt. Lett. **31**(9), 1259 (2006).
[9]B. Lahiri, S. G. McMeekin, A. Z. Khokhar, R. M. De La Rue, and N. P. Johnson, Opt. Express **18**(3), 3210 (2010).
[10]R. Singh, W. Cao, I. Al-Naib, L. Cong, W. Withayachumnankul, and W. Zhang, Appl. Phys. Lett. **105**(17), 171101 (2014).
[11]E. Cubukcu, S. Zhang, Y. S. Park, G. Bartal, and X. Zhang, Appl. Phys. Lett. **95**(4), 043113 (2009).
[12]B. Lahiri, A. Khokhar, R. De La Rue, S. McMeekin, and N. Johnson, Opt. Express **17**(2), 1107 (2009).
[13]D. H. Williams and I. Fleming, *Spectroscopic Methods in Organic Chemistry*, 2nd ed. (McGraw Hill Publications, 1973), Chap. 2.
[14]J. Kischkat, S. Peters, B. Gruska, M. Semtsiv, M. Chashnikova, M. Klinkmüller, O. Fedosenko, S. Machulik, A. Aleksandrova, G. Monastyrskyi, Y. Flores, and W. T. Masselink, Appl. Opt. **51**, 6789 (2012).
[15]C. Wochnowski, S. Metev, and G. Sepold, Appl. Surf. Sci. **154**, 706 (2000).
[16]C. Y. Chen and T. J. Yen, J. Phys. D: Appl. Phys. **42**(18), 185402 (2009).
[17]W. J. Padilla, A. J. Taylor, C. Highstrete, M. Lee, and R. D. Averitt, Phys. Rev. Lett. **96**(10), 107401 (2006).
[18]M. Ren, C. Pan, Q. Li, W. Cai, X. Zhang, Q. Wu, S. Fan, and J. Xu, Opt. Lett. **38**(16), 3133 (2013).
[19]M. Piliarik, P. Kvasnička, N. Galler, J. R. Krenn, and J. Homola, Opt. Express **19**(10), 9213 (2011).
[20]B. Lahiri, G. Holland, V. Aksyuk, and A. Centrone, Nano Lett. **13**(7), 3218 (2013).
[21]S. Naidu, V. Murthy, P. Brahman, and C. Pullaiah, Acta Polym. **41**(6), 349 (1990).
[22]I. M. Pryce, Y. A. Kelaita, K. Aydin, and H. A. Atwater, ACS Nano **5**(10), 8167 (2011).